Hindawi
Wireless Communications and Mobile Computing
Volume 2023, Article ID 9785285, 1 page
https://doi.org/10.1155/2023/9785285

Retraction

Retracted: Design and Implementation of a Radioactive Source Intelligent Search Robot Based on Artificial Intelligence Edge Computing

Wireless Communications and Mobile Computing

Received 17 October 2023; Accepted 17 October 2023; Published 18 October 2023

This article has been retracted by Hindawi following an investigation undertaken by the publisher [1]. This investigation has uncovered evidence of one or more of the following indicators of systematic manipulation of the publication process:

(1) Discrepancies in scope
(2) Discrepancies in the description of the research reported
(3) Discrepancies between the availability of data and the research described
(4) Inappropriate citations
(5) Incoherent, meaningless and/or irrelevant content included in the article
(6) Peer-review manipulation

The presence of these indicators undermines our confidence in the integrity of the article's content and we cannot, therefore, vouch for its reliability. Please note that this notice is intended solely to alert readers that the content of this article is unreliable. We have not investigated whether authors were aware of or involved in the systematic manipulation of the publication process.

Wiley and Hindawi regrets that the usual quality checks did not identify these issues before publication and have since put additional measures in place to safeguard research integrity.

We wish to credit our own Research Integrity and Research Publishing teams and anonymous and named external researchers and research integrity experts for contributing to this investigation.

The corresponding author, as the representative of all authors, has been given the opportunity to register their agreement or disagreement to this retraction. We have kept a record of any response received.

References

[1] P. Wang, Z. Gao, Y. Li, L. Zeng, and H. Zhong, "Design and Implementation of a Radioactive Source Intelligent Search Robot Based on Artificial Intelligence Edge Computing," *Wireless Communications and Mobile Computing*, vol. 2022, Article ID 3940348, 12 pages, 2022.

Hindawi
Wireless Communications and Mobile Computing
Volume 2022, Article ID 3940348, 12 pages
https://doi.org/10.1155/2022/3940348

Research Article

Design and Implementation of a Radioactive Source Intelligent Search Robot Based on Artificial Intelligence Edge Computing

Pin Wang,[1] Zhijian Gao,[2] Yimin Li,[3] Lingyu Zeng,[1] and Hongmei Zhong[1]

[1]*School of Mechanical and Electrical Engineering, Shenzhen Polytechnic, Shenzhen, 518055 Guangdong, China*
[2]*Guangdong Key Laboratory of Intelligent Information Processing and Shenzhen key Laboratory of Media Security, Shenzhen, 518060 Guangdong, China*
[3]*Industrial Training Centre, Shenzhen Polytechnic, Shenzhen, 518055 Guangdong, China*

Correspondence should be addressed to Yimin Li; liyimin@szpt.edu.cn

Received 9 March 2022; Revised 19 April 2022; Accepted 27 April 2022; Published 17 May 2022

Academic Editor: Rashid A Saeed

Artificial intelligence is a very broad science, which consists of different fields, such as machine learning, and computer vision. In recent years, the world nuclear industry has developed vigorously. At the same time, incidents of loss of radioactive sources also occur from time to time. At present, most of the search for radioactive sources adopt manual search, which is inefficient, and the searchers are vulnerable to radiation damage. Sending a robot to the search an area where there may be an uncontrolled radioactive source is different. Not only does it improve efficiency, it also protects people from radiation. Therefore, it is of great practical significance to design a radioactive source search robot. This paper mainly introduces the design and implementation of a radioactive source intelligent search robot based on artificial intelligence edge computing, aiming to provide some ideas and directions for the research of radioactive source intelligent search robot. In this paper, a research method for the design and implementation of a radioactive source intelligent search robot based on artificial intelligence edge computing is proposed, including intelligent edge computing and gamma-ray imaging algorithms, which are used to carry out related experiments on the design and implementation of radioactive sources, an intelligent search robot based on edge computing. The experimental results of this paper show that the average resolution of the radioactive source search robot is 90.55%, and the resolution results are more prominent.

1. Introduction

The nuclear industry is a comprehensive industrial sector for the development and utilization of nuclear energy, also known as the atomic energy industry. With the development of the industry, a large number of radiation sources and radioactive sources will be produced. It is an industry created and developed in the last century and a high-tech strategic industry. In addition to nuclear power, which is booming worldwide, an important branch is the application of isotopes and nuclear technology, which is another important aspect of nuclear energy serving the national economy and people's lives. The use of nuclear technology has become quite popular. In addition to nuclear power, radioactive sources are also widely used in other fields of industry, as well as in agriculture, medical treatment, scientific research, and other industries. They have been successfully used in equipment flaw detection, radiation breeding, sewage treatment, and medical diagnosis, and during the development of new materials and archeology, it can be said that the production and life of modern society are inseparable from the application of radio sources.

Artificial intelligence is a branch of computer science that attempts to understand the nature of intelligence and produces a new type of intelligent machine. Artificial intelligence is also constantly simulating, extending, and expanding human intelligence. Research in this field includes robotics, language recognition, image recognition, natural language processing, and expert systems. It is conceivable that the technological products brought by artificial intelligence in the future will be the "containers" of human intelligence.

At present, the search for radioactive sources within a certain range mainly relies on professional staff holding monitoring equipment and wearing protective equipment for manual searches. To ensure the health and safety of searchers and avoid prolonged exposure to radiation, multiple groups of searchers are generally used to enter the radiation field in batches to search, which requires a lot of time and manpower. The radioactive source search robot originated in Japan, where the supply of electric energy is highly dependent on nuclear power. And radiation will cause great harm to human health, such as damage to human skin and vision. The currently used robots can only detect radiation intensity and cannot search for radioactive sources autonomously, so they are called radiation detection robots. In recent years, the technology of intelligent robots has developed rapidly. The use of robots to search for radioactive sources instead of humans can effectively prevent searchers from being exposed to ionizing radiation, which is of great significance.

Liu et al.'s research found that IoT-based services benefit from the cloud, which provides almost unlimited functions such as storage, processing, and communication. However, for mobile users, how to receive computing from the cloud through satisfactory quality of service (QoS) settings still faces challenges. Liu et al. use edge computing to study computing offload, but if the power is insufficient, the local edge server may not be able to complete the task. Liu et al. used operators and edge server users interactively. They designed two computing offloading algorithms to reduce delay and complexity. However, the scholars did not describe the specific solution, nor did they reflect the advantages of the method; in addition, by considering edge server owners to dynamically join or not perform calculated diversion to expand related research work, the steps of this research method are cumbersome, which is not conducive to popularization in practice [1]. Fan et al. have studied a UAV communication system with mobile edge computing (MEC). Under certain resource conditions, by jointly optimizing the UAV's flight trajectory, task allocation, and CPU calculation speed, the energy consumption of the entire system can be improved and can minimize constraints. From this, Fan et al. derive the energy consumption model for data processing and then obtain the energy consumption model flight of the fixed-wing UAV. Fan et al. apply discrete linear state-space approximation technology to obtain an approximate optimization problem and then convert nonconvex constraints into convex constraint linearization and propose a rough optimization algorithm based on the concave-convex process. This study lacks experimental data support and is weakly persuasive [2]. Durresi et al. believe that protecting the environment from multiple threats is an issue that cannot be ignored at the moment. Durresi et al. proposed an edge computing-based security architecture for collecting sensor information in real time. In their proposed solution, users would combine the use of smartphones and IoT devices. However, the scholars have no specific experimental data and experimental objects, so the conclusion drawn is very low. [3].

The innovations of this paper are as follows: (1) make a detailed introduction of the division and definition of radioactive source search area; (2) proposed the design of horned hummingbird target detection algorithm; and (3) designed a radioactive source search robot system based on the horned hummingbird target detection algorithm. These above research methods and designed systems are not covered in previous studies.

2. Research Method of Design and Implementation of Intelligent Searching Robot for Radioactive Sources Based on Edge Computing

2.1. Overview of Edge Computing

2.1.1. AI-Based Edge Computing. Unprecedented amounts of data, coupled with breakthroughs in artificial intelligence, have made the use of deep learning techniques possible. Edge computing enables machine learning algorithms to be deployed at the edge of the network. Edge computing refers to an open platform that uses the core network, computing, storage, and application capabilities near the object or data source to provide the nearest end services nearby.

Traditional IoT technology is intelligently integrated in the data center, and edge devices play a supporting role. In the industrial Internet of Things, if the client device wants to obtain the decision result, the industrial sensor must first send the collected data to the data center, and then the data center will perform unified calculation processing and analysis and then return the processing result to the user side [4]. However, even if all users are in the same area or even the same place, they must communicate with a long-distance data center to achieve the above functions [5]. This method will not only cause delay but also greatly increase the probability of network congestion, thereby reducing the performance of the entire system. At the same time, since all information must be transmitted to the public data center (cloud), it is easy to cause information leakage, and the data security risk of special information will greatly increase [6].

The European Telecommunications Standards Institute defines mobile edge computing as providing IT service environment and cloud computing capabilities at the edge of the mobile network. That is to say, the service is closer to the user, and the calculation, storage, caching, and communication process originally uploaded to the cloud are transferred to the edge and realized on the neighboring base station, routers, and even mobile phones [7]. Compared with cloud computing, edge computing has three advantages: first of all, edge computing improves user service quality and provides users with more convenient and efficient services; secondly, edge computing can greatly improve data processing efficiency, reduce latency and response time, enable users to obtain the most useful information in the shortest time; and lastly, edge computing can improve network efficiency, reduce user terminal and cloud communication, save backbone network bandwidth pressure, reduce core network energy consumption, avoid network congestion, protect privacy and security, and avoid information leakage when private information is uploaded to cloud [8, 9].

2.1.2. Intelligent Edge Computing. In traditional industrial automation, researchers have summarized problems and solutions through a large number of research and development and let computer equipment help humans to complete mass production according to the set rules [10]. Many of the data that need to be processed in the past are structured data, and the rules can be found to maintain and manage it through Excel or some simple data processing. In the future, the Internet of Things will generate increasingly unstructured data [11]. In the face of high-dimensional complex tasks, the current edge processing capabilities cannot meet people's needs. As an emerging technology, artificial intelligence enables machines to simulate humans to learn, judge, make decisions independently, and perform complex calculations quickly. The more complex the problem, the longer it takes machine learning to deal with the problem. In real life, in some special fields, such as industrial or medical fields, too long processing time is fatal, so artificial intelligence must be introduced into edge computing with strong real-time processing capabilities [12].

To cater to customer needs in the era of big data, the concept of mass production in traditional industrial fields no longer applies. To meet the production requirements of small batches with short cycle and diversified changes, the idea of machine learning, decision tree, and feature engineering is used as inspiration, and the task is decomposed from the perspective of feature data flow [13], select feature data streams related to task decision-making, construct a feature data stream group of the task, and filter out decision-independent data at the same time, avoid the transmission overhead of decision-independent data, and reduce cloud pressure. To improve the utility of the entire system, each edge device must have data collection, analysis and calculation, communication, and the most important intelligent decision-making capabilities [14]. Specifically, in the intelligent edge computing architecture, multiple industrial sensors serve as users to receive different characteristic data and form the characteristic data stream of the characteristic. Consider multiple task sets, each task contains several characteristic data streams to form its characteristic data stream group [15]. If you want to complete a task decision, you must process all characteristic data streams corresponding to the task in a unified manner, complete it locally, or unload it to a designated server for calculation. The cloud is responsible for collecting all feature data in a specific period, training and generating corresponding decision trees according to multiple task requirements, and placing the trained model on the MEC server. The MEC server can use the trained model to make decisions on the tasks of these own models and return the decision results to the client to share the pressure of cloud computing [16]. It can be seen that the relationship between traditional edge computing and AI-based edge computing is interrelated and complementary.

2.2. Gamma-Ray Imaging Algorithm. Gamma rays are also called gamma rays, which belong to high-energy electromagnetic radiation, with energy ranging from tens of thousands of electron volts to millions of electron ford. It has an important role in identifying atomic isotopes. Gamma rays have extremely short wavelengths and have obvious particle characteristics, so they are also called photons [17]. It is generally believed that the generation mechanism of gamma rays is accompanied by the occurrence of alpha or beta decay in the nucleus and when the positive and negative particles annihilate. As the nucleus decays or undergoes a nuclear reaction, the light emitted from the nucleus through the deexcitation process of the nucleus has a characteristic spectrum. Therefore, the gamma-ray spectrum can reflect the characteristics of the nucleus, which can be used to identify various isotopes of the same element [18]. The advantage of gamma-ray imaging algorithm is that its operation process is not complicated, and the imaging efficiency is high.

3. Photoelectric Effect

When the gamma ray enters the medium, because of the interaction with the atoms in the medium, its energy is completely given to a shell electron, which is absorbed by the atom. The shell electron becomes a photoelectron and flies out of the atom, which is called the photoelectric effect. As shown in Figure 1.

Photoelectrons have different probabilities to be generated from electron layers such as the K and L layers of atoms. The K layer has the greatest probability of generating photoelectrons [19]. When the originally bound electron leaves the orbit, a hole is left in its original position. At this time, there will be outer electrons to fill the position. The energy difference between the two is emitted in the form of X-rays. The released energy is absorbed by the outer electrons, which causes the outer electrons to break away from the orbital bond and escape the atoms, which is called Auger electrons. The atom emits X-rays and Auger electrons to return to the ground state from the excited state [20, 21]. According to calculation, when $h\nu << m_e c^2$, the expression of the absorption coefficient A of the photoelectric effect in the μ_γ^K layer is

$$\mu_\gamma^K = (32)^{1/2}\alpha^4\left(\frac{m_e c^2}{h\nu}\right)^{3.5} NZ^5\sigma_{Th} \propto NZ^5\left(\frac{1}{h\nu}\right)^{3.5}. \quad (1)$$

Among them, the fine structure constants $\alpha = 1/137$, $\sigma_{Th} = 6.65 \times 10^{-25} cm^2$, and the number of atoms per unit volume is N.

When $h\nu >> m_e c^2$, the following formula exists:

$$\mu_\gamma^K = 1.5\alpha^4\left(\frac{m_e c^2}{h\nu}\right) NZ^5\sigma_{Th} \propto NZ^5\left(\frac{1}{h\nu}\right). \quad (2)$$

4. Electron Pair Effect

When the gamma photon passes around the nucleus, due to the Coulomb force, the gamma photon is converted into one positive and one negative two electrons. This process is called the electron pair effect [22]. Since electrons have kinetic energy in addition to static energy, it is obvious that the energy of the incident gamma photon must be greater than twice the electron energy, which is $h\nu > 2m_e c^2 (1.02MeV)$. If $h\nu = 2m_e c^2$, it

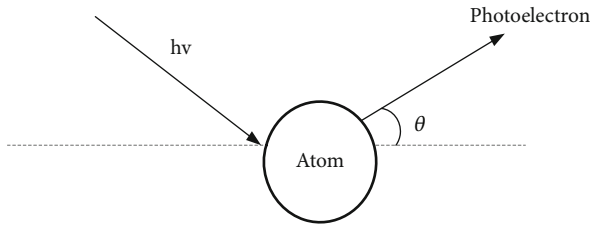

Figure 1: Schematic diagram of photoelectric effect.

means that all gamma photon energy is absorbed by the nucleus [23]. This energy conversion can be expressed as

$$h\nu = \left(E_e^+ + m_e c^2\right) + \left(E_e^- + m_e c^2\right). \quad (3)$$

5. Compton Scattering

The required energy for Compton scattering is between the photoelectric effect and the electron pair effect. When the energy of the gamma ray is close to 1.02 MeV, the probability of the Compton effect will increase sharply, and the probability of the photoelectric effect will decrease. The Compton effect is a more complicated one. The principle of action is that gamma rays enter the atomic range. After the photon undergoes an inelastic collision with the outer electron, the outer electron becomes a recoil electron, and the photon itself becomes the speed direction.

Generally speaking, the attenuation of gamma rays in matter is mainly carried out through the three methods mentioned above, but the proportions of the three methods are different under different conditions, because different methods have different effects on gamma-ray imaging in different situations. To achieve the goal of using gamma rays for radiation imaging, the above three decay methods are selected according to the actual situation in this article. The photoelectric effect accounts for the low energy and high atomic number region. Advantage Compton scattering is dominant in the middle energy and low atomic number region, and the electron pair effect is dominant in the high energy and high atomic number region. Therefore, based on the consideration of detection efficiency, we try to avoid the interference of Compton scattering, and the detectors mostly use materials with relatively large atomic numbers, such as NaI (Tl).

6. Experiments on the Design and Implementation of an Intelligent Search Robot for Radioactive Sources Based on Edge Computing

6.1. Search Area Division and Definition. When conducting a random search of radioactive sources, for the problem of radioactive source search in a large area, the search area should be reduced to improve the search speed and efficiency. If the random search range is too large, there may be a large number of low radiation dose signal parts, which requires a lot of manpower, material resources, and time to collect grid node data, which not only increases the length of the search path but also is not conducive to fast searching for radioactive sources. If the random search area is too small, it may cause some radioactive sources to be missed, which is undesirable in the search problem, so it is essential to select the random search area appropriately.

If the search area is large and irregular, the search area can be divided into several rectangular search areas as large as possible and then search for each rectangular area. Therefore, it may be assumed that the search area is a rectangular area. If the rectangular search area is larger, a smaller effective search range can be determined in the rectangular area, so that the radioactive source is within this range and every point in the range can be monitored. The radiation dose value is to ensure that the search can be carried out smoothly and improve the search speed.

7. Large Area Meshing Algorithm

For a predetermined larger rectangular search area, $D = \{(x, y) | 0 \le x \le a^*,\ 0 \le y \le b^*\}$. To determine the maximum width R of a suitable grid division, it is necessary to ensure that the radiation source must be able to detect the radiation dose value in the rectangular area with a distance of R. The length a^* and width b^* of the rectangular area will be much larger than R. Then mesh the large rectangular area D. Enter the divided width R to find $n = [a^*/R]$, $m = [b^*/R]$.

Insert equal points, let $x_0 = 0$:

$$x_i = x_0 + i \cdot R \; i = 1, 2, \cdots, n-1 \quad x_n = a^*. \quad (4)$$

Let $y_0 = 0$:

$$y_i = y_0 + j \cdot R \quad j = 1, 2, \cdots, m-1 \quad y_m = b^* \quad (5)$$

Get point set:

$$E_n \times E_m = \left\{ \left(x_i, y_j\right) | i = 1, 2, \cdots, n \; j = 1, 2, \cdots, m \right\}. \quad (6)$$

Collect the radiation dose value (x_i, y_j) of grid node $f(x_i, y_j), i = 1, 2, \cdots,\ n\, j = 1, 2, \cdots, m$.

8. Definition of Search Area

The definition of the search area refers to selecting nodes whose radiation dose exceeds a threshold in a larger rectangular area and enclosing the eligible nodes in the search area. For $\forall (x_i, y_j) \in E_n \times E_m$, the indicative function has the following formula:

$$z\left(x_i, x_j\right) = \begin{cases} 1, & f\left(x_i, x_j\right) \ge kM, \\ 0, & f\left(x_i, x_j\right) < kM, \end{cases} \quad (7)$$

where M is the order of magnitude of the radiation dose of the radioactive source to be searched, k is an adjustable parameter, and generally, $k \in [0.1, 0.5]$. Taking max $\{x_i, x_j\}$ and min $\{x_i, x_j\}$ as the upper and lower bounds in the X direction of the rectangular area and max $\{y_i, y_j\}$ and min

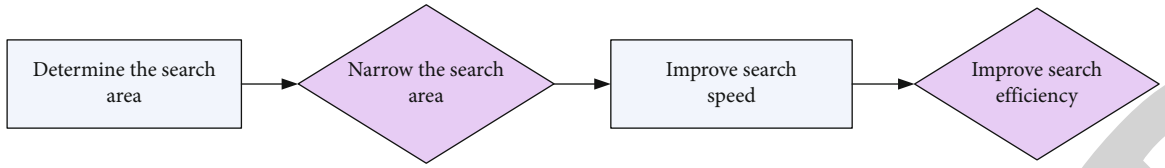

Figure 2: Random search algorithm flow for radioactive sources.

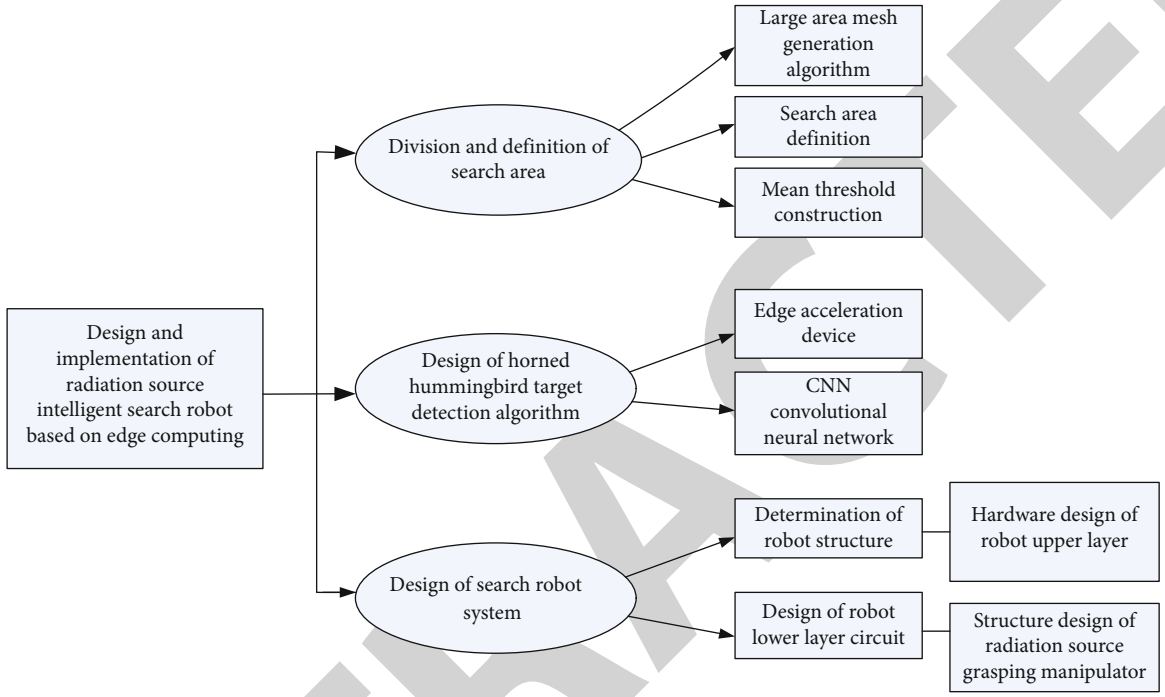

Figure 3: The experimental process of this article.

$\{y_i, y_j\}$ as the upper and lower bounds in the Y direction of the rectangular area, respectively, the search area is obtained.

9. Mean Threshold Structure

For multiple radioactive sources of the same quality and equivalent, the average value of the maximum points in the monitoring area can be used to construct the threshold function. Suppose the maximum points in the monitoring area are, respectively $A_1, A_2, \cdots, A_n$, and let the threshold function be

$$t = k \cdot \frac{1}{n} \sum_{i=1}^{n} A_i, \tag{8}$$

where k is an adjustable parameter, and generally, $k \in [0.6, 1]$. When the radiation dose value $f(x_i, y_j) \geq t$ of the maximum point is searched, the maximum point is the radioactive source point: otherwise, it is not the radioactive source.

The overall flow of the random search algorithm for the radioactive source is shown in Figure 2.

9.1. Design of Target Detection Algorithm for Horned Hummingbird. The design of the diagonal hummingbird object detection algorithm mainly includes three main parts: edge acceleration device setup, convolutional neural network-based image processing, and algorithm optimization. The procedure is performed in the following sections.

9.1.1. Edge Acceleration Device Setup. The edge acceleration device mainly uses its specific hardware circuit to realize the accelerated reasoning of the neural network. The neural network supported by Horned Hummingbird is mainly a CNN convolutional neural network, which is used for computer vision inference. Here, it is used to infer the hot optical fusion image output by the gamma camera and identify road obstacles in front of the robot, and cooperate with Lidar for autonomous obstacle avoidance navigation

The SSD network is mainly used for target detection. The one-stage idea is adopted to improve the detection speed, and the anchors are combined with feature extraction, and then the action classification and border regression of the corresponding layer are calculated and scored. This method can compensate for the lack of accuracy of Mobile Net. While improving the detection accuracy, it can also increase the real-time detection. The SSD network continues to add a total of four layers of Conv8, Conv9, Conv10, and Conv11 to extract higher-level semantic information. In each stage operation, the network contains multiple convolutional layer operations, and each convolutional layer operation is basically a

Table 1: The radius of the photon contribution area when the three energies reach the corresponding flux ratio.

Energy (MeV)	60% flux ratio	80% flux ratio	85% flux ratio	90% flux ratio
1.460	5.1	10.6	14.9	23.4
1.765	5.3	10.9	15.3	27.5
2.614	5.4	11.1	15.2	26.2

small convolution. The entire model uses the yolo model trained on the VOC dataset, with a total of 20 object tags.

9.1.2. CNN Convolutional Neural Network. After the computer obtains the image, it processes the image into a two-dimensional data matrix, obtains the required knowledge according to various algorithms, obtains the classified network structure, and output the network structure target image. Convolutional neural networks provide a way to extract feature values using the idea of convolution.

(1) Convolutional Layer. I denotes the input feature map and K denotes the convolution kernel. The convolution operation can be represented by the following formula:

$$O(y,x)=\sum_{u=1}^{k_1}\sum_{v=1}^{k_2}K(u,v)I(y+u,x+v,i). \tag{9}$$

The feature map is

$$O(y,x,j)=\sum_{i=1}^{c_1}\sum_{u=1}^{k_1}\sum_{v=1}^{k_2}K(u,v,i)I(y+u,x+v,i,j). \tag{10}$$

Sigmoid function expression is

$$f(x)=\frac{1}{1+e^{-x}}. \tag{11}$$

The Tanh function expression is

$$Tanh(x)=\frac{1-e^{-2x}}{1+e^{-2x}}. \tag{12}$$

The ReLu function expression is

$$y=\begin{cases}0, & (x<0),\\ x, & (x\geq 0).\end{cases} \tag{13}$$

(2) Optimization Method. The best way is to figure out how to minimize the loss. If a dataset D is given, the goal of optimization is the average of all data losses for D, that is, the average loss of the minimum value. There is the following formula:

$$L(W)=\frac{1}{|D|}\sum_{t}^{|D|}f_w\left(x^{(t)}\right)+\lambda_r(W), \tag{14}$$

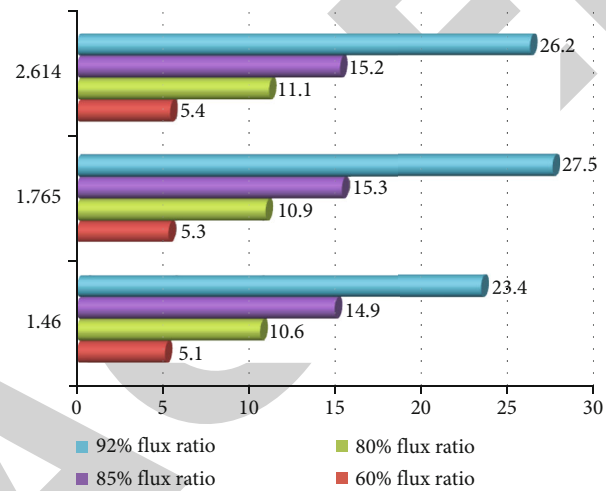

Figure 4: The radius of the photon contribution area when the three energies reach the corresponding flux ratio.

where $L(W)$ is the calculated minimum average loss. A random subset N of the dataset is shown in

$$L(W)\approx\frac{1}{N}\sum_{t}^{N}f_w\left(x^{(t)}\right)+\lambda_r(W). \tag{15}$$

9.2. Search Robot System Design

9.2.1. Determination of the Structure of the Robot. The crawler walking mechanism is the most suitable walking mechanism for the radioactive source search robot. There are three types of commonly used crawler walking mechanisms, namely, double crawler mechanism, four crawler mechanisms with front swing arms, and six crawler mechanisms with swing arms both front and rear. The four-track and six-track mechanisms are large in size and weight and have complex structures. Usually, there is no need to cross trenches in the process of searching for radioactive sources. To reduce the complexity of the mobile platform, the mobile platform adopts a double-track mechanism to make it better terrain adaptability. At the same time, taking into account the position of the center of gravity of the car body, to prevent the car from tipping over during the grasping task, the rear dual motor drive is adopted to ensure that the center of gravity of the car is always located in the middle of the car body. As industry and services continue to grow, there is a growing demand for such search robots.

Table 2: Average number of moving steps in random search.

Experiment	Search random starting points	The number of times the correct source was found	Average number of steps of search success
1	1000	1000	489
2	10000	10000	491
3	100000	100000	492

Table 3: Dynamic obstacle avoidance test distance.

	Minimum distance (cm)	Maximum distance (cm)	Average distance (cm)
Cartons	13.1	19.6	14.3
Plastic blocks	14.2	15.8	14.5
Rubber tires	13.6	15.1	14.1
Metal objects	15.3	17.2	15.4
Clothing	12.7	14.3	13.1
Vitreous	17.0	23.2	16.9

Table 4: Dynamic obstacle avoidance test time.

	Minimum time (s)	Maximum time (s)	Average time (s)
Cartons	16.2	32.5	27.6
Plastic blocks	17.3	29.4	25.1
Rubber tires	16.9	28.7	23.1
Metal objects	18.1	30.8	24.4
Clothing	16.1	27.6	23.5
Vitreous	21.4	40.5	32.6

9.2.2. The Upper Hardware Design of the Robot. The upper part of the robot includes Lidar system, Raspberry Pi single-board computer, gamma-ray imager, and horned hummingbird edge acceleration board. To balance the battery life and performance of the robot, traditional large-scale PC computers cannot be used, and single-board computers with relatively low power consumption but still outstanding performance are required. The Raspberry Pi single-board computer is finally selected for the comprehensive development environment resources. The Raspberry Pi single-board computer is an educational mini PC designed and released by the British Raspberry Pi Foundation. Its latest model 3B+ uses Broadcom's 64-bit 1.4GHz quad-core CPU BCM2837B0, comes with 1GDDR2 running memory, onboard Bluetooth 4.2 and 802.11AC wireless dual-band WiFi, can be powered by external HAT Ethernet Poe, and can be stored via external storage operating system required for card loading.

9.2.3. The Lower Circuit Design of the Robot. In addition to the mechanical structure, the robot system also requires hardware circuit design. In addition to the gamma-ray imaging system and the angular hummingbird edge computing board (upper device) mentioned above, the robot's own hardware circuit also needs to be designed, including the lower layer: power supply Management, stm32 minimum system, motor drive, IMU (Inertial Measurement Unit), OLED display, remote control, steering gear control, voltage detection, ultrasonic obstacle avoidance, and expansion interface; and upper hardware equipment: Lidar, Raspberry Pi Single board computer and depth camera.

9.2.4. Structural Design of the Radioactive Source Grabbing Robot Arm. From the perspective of versatility, the robot arm generally chooses 6 degrees of freedom, but from the perspective of economy and practicability, the degree of freedom of the robot arm should be selected according to the requirements of the specific work task, to meet the requirements of the work task. The lower degrees of freedom should be as few as possible. The radioactive source grabbing manipulator is installed on a crawler robot platform. The mobile platform can provide 2 degrees of freedom, and a 4 -degree-of freedom manipulator can complete the task of grabbing the radioactive source. Therefore, the radioactive source grabbing manipulator is designed as 4 degrees of freedom arm.

When the general industrial robot end effector reaches a certain point in the working space, the first three joints determine the position of the end, and the last three joints determine the posture of the end.

The radioactive source grasping manipulator works on a small robot mobile platform. The driving and transmission components that can be placed on the mobile platform are limited. Therefore, a structure with simple driving and transmission and a large ratio of working space to volume should be considered. In the form of joints, since the output of the

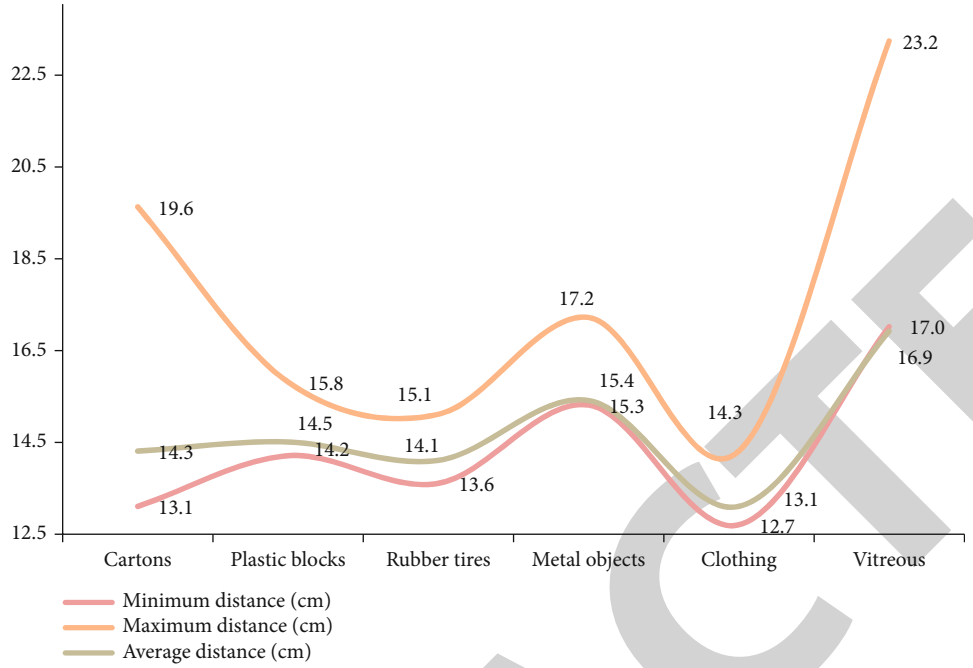

Figure 5: Dynamic obstacle avoidance test distance.

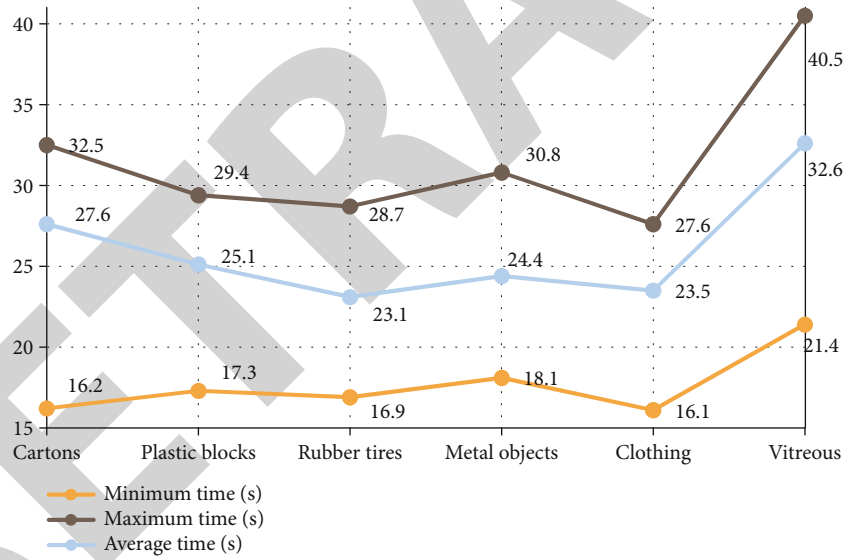

Figure 6: Dynamic obstacle avoidance test time.

Table 5: Autonomous sourcing time at 20 m distance under 15 mCi intensity.

Frequency	Time (s)	Frequency	Time (s)
1	231	6	233
2	245	7	241
3	229	8	239
4	232	9	244
5	237	10	230

motor is rotation, the realization of the sliding pair usually requires more transmission components than the rotating pair. Therefore, it is determined that the radioactive source grasping the robot arm is a joint type or a SCARA type. Further analysis, the robotic arm needs a larger working space above the ground, and the articulated robotic arm can better meet this requirement, and the radioactive source grasping the robotic arm is finally determined to be an articulated robotic arm. Therefore, it is determined that the first three joints of the manipulator are the base rotary joint, the big

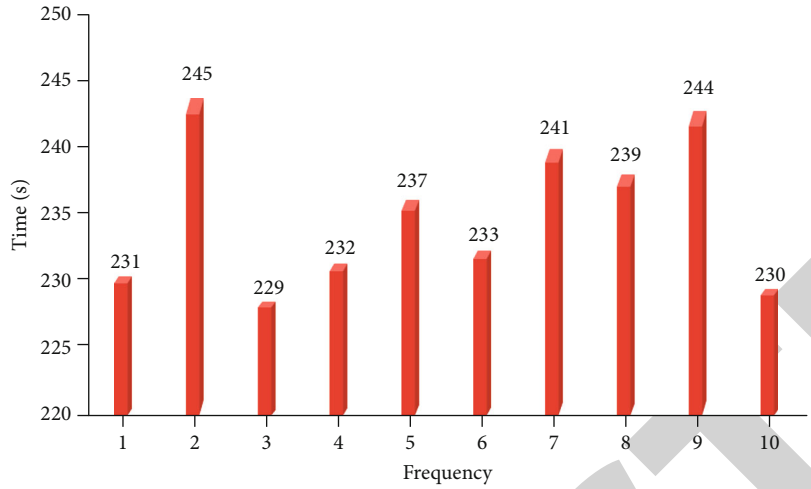

Figure 7: Autonomous sourcing time at 20 m distance under 15 mCi intensity.

Table 6: Robot resolution.

Lab environment	Test line	Single crystal-resolution	FCL crystal-resolution
Natural environment	Midline	87.1%	90.1%
	Sideline	86.4%	91.4%
Lead room	Midline	88.2%	92.5%
	Sideline	86.5%	93.2%
Natural environment	Midline	84.3%	96.3%
	Sideline	89.2%	97.1%
Lead room	Midline	87.4%	94.5%
	Sideline	88.3%	95.7%
Average		87.2%	93.9%

arm pitch joint, and the forearm pitch joint. The fourth joint of the robotic arm is designed as a rotation of the wrist joint.

This part of the experiment proposes that the above steps are used to perform related experiments on the design and implementation of an intelligent search robot for radioactive sources based on edge computing. The specific process is shown in Figure 3.

10. Design and Implementation of an Intelligent Searching Robot for Radioactive Sources Based on Edge Computing

10.1. Experiment and Test Analysis

(1) According to the analysis and calculation, the detection range when the flux of gamma photons emitted from the ground accounts for 90%, 85%, and 80% is obtained. The calculation results are shown in Table 1 and Figure 4

Taking the energy of 1.460 MeV as an example, if the photon flux accounts for 90%, the corresponding sampling area is a circular area with a radius of 23.4 m and an area of about 1,719 square meters. Based on this, it is considered that the gamma-ray imaging algorithm is in environmental radioactivity. The data during the measurement represents the average radioactivity distribution within a radius of about 23 m centered on the robot. It can be seen from the chart that when the proportion of photon flux increases from 80% to 90%, the radius of the photon contribution area increases by 12.8 m, and the corresponding radiation survey area increases from 353 square meters to 1,719 square meters, to obtain 10% more the number of gamma samples is increased by nearly five times. This will inevitably affect the efficiency of sampling and cost a lot of time. Therefore, in actual work, a suitable sampling area should be pursued for the energy of interest. It is recommended to use the sampling radius when the photon flux accounts for 80%.

(2) Randomly generate a search starting point on the plane of the search area. Starting from the starting point, search for the maximum value of the four points up, down, left, and right of the point. If you find a larger starting point, move one step and count once, and then use this point as starting point, do not compare the left and right four nodes one by one, look for the major nodes, move one step, and then count sequentially, and proceed in sequence until

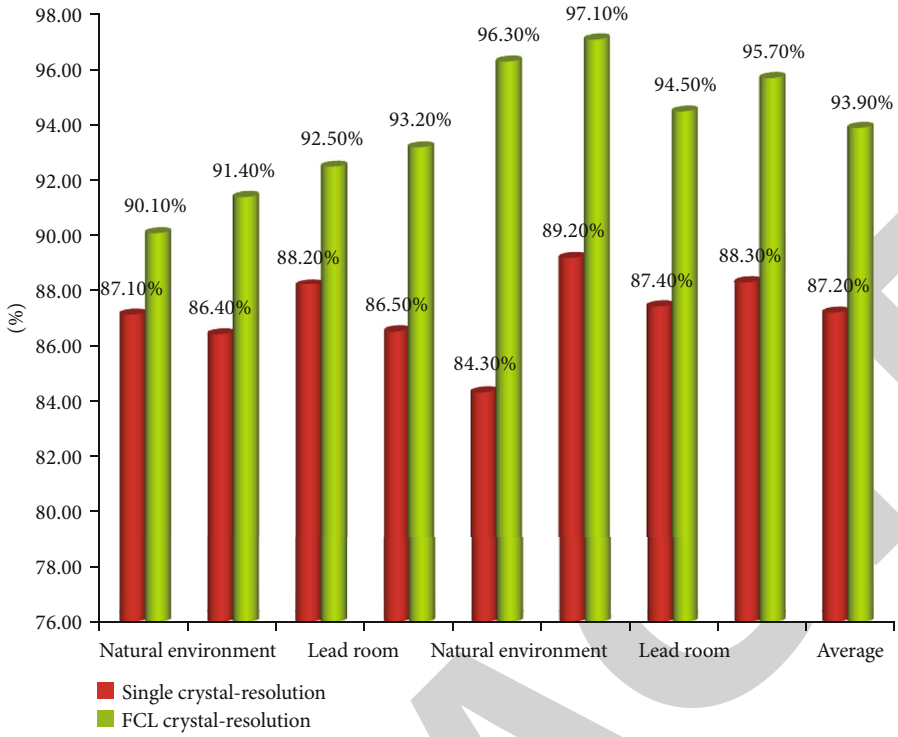

Figure 8: Robot resolution.

the value of the upper, lower, left, and right points are less than this point, that is, stop random search and output the record. In the number of moving steps in the search, find the average number of moving steps per random search performed in the simulation experiment. There are three groups of simulation experiments, and each group randomly generates 1,000, 10,000, and 100,000 starting points for the search and records the number of steps moved by each random search. The details are shown in Table 2

Through simulation experiments, it can be seen that in the 1000 × 1000 grid data, the average number of successful moving steps is about 491 steps.

(3) Select common obstacles for ten robot avoidance experiments, such as paper boxes, plastic blocks, rubber tires, metal objects, clothing, and glass bodies, check the distance recorded by the Lidar in rosbag, and use a stopwatch to time, as shown in Tables 3 and 4 and as shown in Figures 5 and 6

It can be seen from the above chart that, due to the limitations of the site's terrain, the aisle width excludes the width of the robot and the width of the obstacles, and the idle distance is narrow. The restrictions on the robot are very large. The robot may make multiple posture adjustments to move forward and backward in one pass, which is waste a lot of time. It can be seen from the data sheet that the largest fluctuation is the glass obstacle. This is mainly due to the weak reflection of the glass on the laser. The laser will transmit or scatter and escape, resulting in the inability to receive the echo signal, resulting in failure to detect the obstacle. In this case, the camera is also difficult to deal with. In practical applications, you should try to avoid glass-like objects. The overall effect of other objects is well tested.

(4)In the experiment process of this article, the radioactive source was uniformly placed in the initial field of view of the gamma camera. In the case of a known environmental map, 5 obstacles were randomly placed on the road with a distance of 15 mCi, Cs-137, and 20 m. Record the timing of the robot from turning on to moving on within 20 cm of the radioactive source, perform ten repeated tests, and count the specific situation of the source search time, as shown in Table 5 and Figure 7

It can be seen from the test results that the average search time for a 20 m interval radioactive source is 236.1 seconds.

10.2. Robot Resolution Analysis. To thoroughly understand the resolution change of the radioactive source search robot, it is necessary to conduct an experimental test of resolution and stability before using the robot for experiments. This test uses a 137Cs radioactive source with an energy peak of 1.460 MeV, a gamma digital multichannel energy spectrum acquisition card, and the corresponding energy spectrum test software. The resolution test of the single crystal system and the resolution test of the full box crystal system are carried out. The specific results are shown in Table 6 and Figure 8.

From the calculation of the data in the chart, it can be seen that the average resolution of the radioactive source search robot is 90.55%, which has a high resolution and can perform radioactive source search operations well.

11. Conclusions

Due to the vigorous development of the nuclear industry and the frequent occurrence of radiation accidents, the demand for radioactive source search robots has become increasingly urgent. Radiation can cause harm to human health, ranging from weakness, coughing, and fever, to organ failure or even death. For large-scale nuclear power plant accidents, the accident area will have extremely high radiation intensity, and large doses of radiation cannot be isolated by wearing radiation protection suits. If manual treatment is performed, it will cause great harm to humans, so humans cannot come to the accident site for treatment and treatment.

For small-scale radioactive source loss accidents, because the location of the radioactive source is not known, the location of the radioactive source cannot be accurately determined, so the manual search for out-of-control radioactive sources has low efficiency and high health risks. However, under the same circumstances, the use of radioactive source search robots to deal with radiation accidents will not pose a threat to human health, and its convenient operation and high work efficiency are the first choice for accident handling.

In the initial stage of the research, this paper provides an overview of edge computing, including the application of artificial intelligence in edge computing; proposes gamma-ray imaging algorithms, including photoelectric effect, electron pair effect, and Compton scattering; and then carries out edge computing-based experiments related to the design and implementation of intelligent search robots for radioactive sources, including the division and definition of search areas, the design of horned hummingbird target detection algorithms, and the design of search robot systems.

A major goal of AI research is to enable machines to perform complex tasks that normally require human intelligence. Edge computing based on artificial intelligence can play a large role in the design and implementation of radioactive source intelligent search robots.

Data Availability

Data sharing is not applicable to this article as no datasets were generated or analysed during the current study.

Conflicts of Interest

The authors declare that they have no conflicts of interest.

References

[1] Y. Liu, C. Xu, Y. Zhan, Z. Liu, J. Guan, and H. Zhang, "Incentive mechanism for computation offloading using edge computing: a Stackelberg game approach," *Computer Networks*, vol. 129, no. DEC.24, pp. 399–409, 2017.

[2] L. Fan, W. Yan, X. Chen, Z. Chen, and Q. Shi, "An energy efficient design for UAV communication with mobile edge computing," *China Communications*, vol. 16, no. 1, pp. 26–36, 2019.

[3] M. Durresi, A. Subashi, A. Durresi, L. Barolli, and K. Uchida, "Secure communication architecture for internet of things using smartphones and multi-access edge computing in environment monitoring," *Journal of Ambient Intelligence & Humanized Computing*, vol. 10, no. 4, pp. 1631–1640, 2019.

[4] W. Shi, J. Cao, Q. Zhang, Y. Li, and L. Xu, "Edge computing: vision and challenges," *IEEE Internet of Things journal*, vol. 3, no. 5, pp. 637–646, 2016.

[5] M. Satyanarayanan, "The emergence of edge computing," *Computer*, vol. 50, no. 1, pp. 30–39, 2017.

[6] C. Vallati, A. Virdis, E. Mingozzi, and G. Stea, "Mobile-edge computing come home connecting things in future smart homes using LTE device-to-device communications," *IEEE Consumer Electronics Magazine*, vol. 5, no. 4, pp. 77–83, 2016.

[7] B. Liu, Y. Li, Y. Liu, Y. Guo, and X. Chen, "PMC," *Proceedings of the ACM on Interactive Mobile Wearable and Ubiquitous Technologies*, vol. 4, no. 4, pp. 1–25, 2020.

[8] X. Liu, J. Yu, Z. Feng, and Y. Gao, "Multi-agent reinforcement learning for resource allocation in IoT networks with edge computing," *China Communications*, vol. 17, no. 9, pp. 220–236, 2020.

[9] Y. Wu, Q. Liu, R. Chen, C. Li, and Z. Peng, "A group recommendation system of network document resource based on knowledge graph and LSTM in edge computing," *Security and Communication Networks*, vol. 2020, no. 1, 11 pages, 2020.

[10] J. Skirelis and D. Navakauskas, "Performance analysis of edge computing in IoT," *Elektronika ir Elektrotechnika*, vol. 26, no. 1, pp. 72–77, 2020.

[11] X. Zhang, J. Zhang, J. Xiong, L. Zhou, and J. Wei, "Energy efficient multi-UAV-enabled multi-access edge computing incorporating NOMA," *IEEE Internet of Things Journal*, vol. 7, no. 6, pp. 5613–5627, 2020.

[12] N. Saranya, K. Geetha, and C. Rajan, "Data replication in Mobile edge computing systems to reduce latency in Internet of Things," *Wireless Personal Communications*, vol. 112, no. 4, pp. 2643–2662, 2020.

[13] G. Li and J. Cai, "An online incentive mechanism for collaborative task offloading in mobile edge computing," *IEEE Transactions on Wireless Communications*, vol. 19, no. 1, pp. 624–636, 2020.

[14] A. J. Ferrer, J. M. Marquès, and J. Jorba, "Towards the decentralised cloud," *ACM Computing Surveys (CSUR)*, vol. 51, no. 6, pp. 1–36, 2019.

[15] S. Distefano, D. Bruneo, F. Longo, G. Merlino, and A. Puliafito, "Personalized health tracking with edge computing technologies," *BioNano Science*, vol. 7, no. 2, pp. 1–3, 2016.

[16] L. Ogiela, M. R. Ogiela, and H. Ko, "Intelligent data management and security in cloud computing," *Sensors*, vol. 20, no. 12, p. 3458, 2020.

[17] Y. H. Li, K. Zhao, N. Yang, F. Chen, and Q. X. Zhang, "Study on the simulation of missing radioactive source with predictive band method," *Hedianzixue Yu Tance Jishu/Nuclear Electronics & Detection Technology*, vol. 37, no. 2, pp. 221–224, 2017.

[18] B. Asvija, R. Eswari, and M. B. Bijoy, "Security threat modelling with Bayesian networks and sensitivity analysis for IAAS virtualization stack," *Journal of Organizational and End User Computing (JOEUC)*, vol. 33, no. 4, pp. 44–69, 2021.

[19] H. Yamanishi, M. Inagaki, and G. Wakabayashi, "A survey of environmental radioactive cesium due to the accident of TEPCO Fukushima Daiichi NPP in Kawamata-machi, Fukushima-ken," *Journal of Smart Processing*, vol. 4, no. 6, pp. 268–274, 2015.

[20] H. Lu, Y. Li, M. Chen, H. Kim, and S. Serikawa, "Brain intelligence: go beyond artificial intelligence," *Mobile Networks and Applications*, vol. 23, no. 7553, pp. 368–375, 2018.

[21] A. Revathy, C. S. Boopathi, O. I. Khalaf, and C. A. Romero, "Investigation of AlGaN channel HEMTs on β-Ga2O3 substrate for high-power electronics," *Electronics*, vol. 11, no. 2, p. 225, 2022.

[22] R. J. Spiro, B. C. Bruce, and W. F. Brewer, "Theoretical issues in reading comprehension: perspectives from cognitive psychology, linguistics, artificial intelligence, and education," *Reading Teacher*, vol. 3, pp. 368–373, 2017.

[23] H. Abulkasim, A. Farouk, H. Alsuqaih, W. Hamdan, S. Hamad, and S. Ghose, "Improving the security of quantum key agreement protocols with single photon in both polarization and spatial-mode degrees of freedom," *Quantum Information Processing*, vol. 17, no. 11, pp. 1–11, 2018.